

1
2
3 1 **SILVER NANOPARTICLES-CLAYS NANOCOMPOSITES AS FEED ADDITIVES:**
4 2 **CHARACTERIZATION OF SILVER SPECIES RELEASED DURING *IN VITRO* DIGESTIONS.**
5 3 **EFFECTS ON SILVER RETENTION IN PIGS**
6
7

8 4 **I. Abad-Álvarez¹, C. Trujillo¹, E. Bolea¹, F. Laborda¹, M. Fondevila², M.A. Latorre² and J.R.**
9 5 **Castillo¹**

10
11 6 ¹ *Group of Analytical Spectroscopy and Sensors (GEAS), Institute of Environmental Sciences*
12 7 *(IUCA), University of Zaragoza, Pedro Cerbuna 12, 50009 Zaragoza, Spain.*

13
14 8 ² *Departamento de producción Animal y Ciencia de los Alimentos, Instituto Agroalimentario de*
15 9 *Aragón (IA2), Universidad de Zaragoza-CITA, M. Servet 177, 50013 Zaragoza, Spain*
16
17

18
19 11 **Abstract**

20
21 12 Two different clay nanocomposites, as sepiolite-Ag and kaolinite-Ag, are studied as carriers for
22 13 silver nanoparticles (AgNPs) oral administration as antimicrobial agent in additives for animal
23 14 feed. A three-step digestibility assay, corresponding to stomach, small and large intestine
24 15 simulations, has been followed. Ultrafiltration and asymmetrical flow field-flow fractionation
25 16 (AF4) coupled to UV-Vis absorption and ICPMS detectors have been used for size
26 17 characterisation of the silver species released during the *in vitro* digestibility assays. Less than
27 18 1% of the total silver is released in the stomach simulation step, probably due to the formation
28 19 of silver chloride on the nanocomposite surface. In the case of the intestine simulation, silver
29 20 released increases and tends to form complexes with the enzymes present in the media. A larger
30 21 amount of silver was released from kaolinite-Ag compared to sepiolite-Ag (17 vs. 7 %), probably
31 22 due to a higher retention rate of silver shown by sepiolite, justified by its sorption capacity and
32 23 fibrous structure. No evidences were found about a significant release of silver nanoparticles
33 24 along the *in vitro* assay from any of the two nanocomposites studied. These results have been
34 25 compared to the silver levels found in liver and faeces from weaned pigs fed with these
35 26 supplements for 35 days and followed by basal diet free of silver for 4 weeks in an *in vivo* assay.
36 27 Piglets fed with kaolinite-Ag retained more silver in liver than those receiving sepiolite-Ag, and
37 28 the opposite was observed in faeces, although differences were not statistically significant.
38 29 Silver levels found in muscles were below the limit of detection (0.009 µg Ag g⁻¹) in all cases.
39
40
41
42
43
44
45
46
47
48
49
50

51
52 31 **Keywords:** Ag nanoparticles; digestibility assays; Field Flow Fractionation; ICPMS; clay
53 32 nanocomposites
54
55
56
57
58
59

60
61
62 **33 1. Introduction**
63
64
65

66 35 Antibiotics have been used for decades as growth promoters in animal feed to obtain higher
67
68 36 productive performances. However, this practise can lead to their retention in animal tissues,
69
70 37 with a risk for potential increase of antibiotic resistance processes for consumers of animal
71
72 38 products. Following the ban of antibiotics as growth promoters in the European Union [1], the
73
74 39 research for alternatives has increased. Organic acids, probiotics, prebiotics, essential oils and
75
76 40 plant extracts are some of the most widely used products in poultry and swine production
77
78 41 [2][3][4]. In this context, silver has raised as a potential alternative. Silver in its ionic form
79
80 42 (nitrates, sulphates or chlorides) is an antimicrobial agent for many pathogens [5][6]. The use of
81
82 43 metallic silver in the form of nanoparticles has been also proposed, due to their greater stability,
83
84 44 lower dose required, greater antimicrobial activity and lower toxicity for eukaryotic cells
85
86 45 [7][8][9]. For instance silver nanoparticles have been added to drinking water or adsorbed in
87
88 46 binding agents and included in diets for chickens [10][11] and pigs [12]. The use of silver
89
90 47 nanoparticles has shown to be effective in the reduction of potentially pathogenic organisms
91
92 48 [6][13], although studies on their effect in animal production are scarce. Since it is expected that
93
94 49 silver activity depends on dose and availability though the digestive tract, the form of
95
96 50 administration must be considered.
97
98
99

100 51 Clays are structural components of soil that have been employed for many years as industrial
101
102 52 minerals, with many applications depending on their properties. The most common in the
103
104 53 industry are: kaolinites, smectites and sepiolites [14]. Clays have a high metal sorption capacity
105
106 54 due, among other characteristics, to their physical and chemical stability, their high surface area
107
108 55 and their cation exchange capacity [15][16]. They are used in animal feed for multiple
109
110 56 technological (binding, fluidifying and anti-caking), nutritional (increase in the digestibility of
111
112 57 nutrients, reduction of transit speed), sanitary (gastric and intestinal protection, prevention
113
114 58 against diarrhoea) and environmental applications (reduction of ammonia emissions and bad
115
116
117
118

119
120
121 59 odours). The antibacterial activity of clays is based on the strong adsorption of toxins produced
122
123 60 by bacteria, which leads to a significant reduction in the adhesion of bacteria to the surface of
124
125 61 epithelial cells. Therefore, the composite based on clays and silver nanoparticles may have a
126
127 62 synergistic effect [17], which make them a possible alternative as growth promoter additives
128
129 63 and antimicrobial in animal feed.

131
132 64 The study of transformations suffered by silver-based nanomaterials along the animal digestion
133
134 65 requires the use of diverse approaches. *In vitro* assays assume some simplifications with respect
135
136 66 to *in vivo* systems but can reveal some hints about the potential effects or risk in their use. Some
137
138 67 studies have used *in vitro* digestion models [18][19][20][21][22][23][24][25][26] to monitor
139
140 68 changes of AgNPs after incubation in artificial environments simulating the different digestive
141
142 69 sites. AgNPs and AgNO₃ have been tested at different steps of the digestion process by dynamic
143
144 70 light scattering (DLS) and scanning electron microscopy (SEM) [18][20][22], single particle-ICPMS
145
146 71 [18][19], or transmission electronic microscopy (TEM) [23]. AgNPs have been also detected by
147
148 72 AF4 coupled to UV-Vis [26] and also quantified by UV-Vis absorption spectroscopy in other
149
150 73 studies [22][25][27]. Aggregation of Ag nanoparticles during *in vitro* digestion in presence of
151
152 74 food by small-angle X-Ray scattering has been also described [21]. In most of these studies it has
153
154 75 been concluded that AgNPs undergo different processes of agglomeration [18][19–21][26] and
155
156 76 changes during digestion, so AgNPs would reach the intestine wall. On the other hand, Bove et
157
158 77 al. [22] also determined the fraction of free dissolved ions and silver complexes isolated by
159
160 78 ultrafiltration (UF) and quantified by ICP-AES, similarly to Wu et al [25] measuring ultrafiltrates
161
162 79 by ICPMS. They demonstrated that most of these NPs dissolved as ions, mostly during the
163
164 80 stomach phase, and these ions appeared to be bound to the matrix, so exposure levels were
165
166 81 expected to be like those observed for silver ions. The lack of standardized procedures for these
167
168 82 assays and techniques to measure these processes (dissolution, aggregation, etc.) represent a
169
170 83 limiting factor and can explain the discrepancies observed along these studies.
171
172
173
174
175
176
177

178
179
180 84 The use of additives for animal feeding based on nanocomposites (in this case particles of
181
182 85 kaolinite and sepiolite with silver nanoparticles deposited on the surface) as antimicrobial
183
184 86 agents, requires the study of the potential effects on both human health and the environment.
185
186 87 In this study, the total silver contents in different organs and tissues of pigs treated with these
187
188 88 nanomaterials were determined and related to the different forms of silver found in *in vitro*
189
190 89 digestibility assays.
191
192
193 90 The objective of the present work is to study the transformation suffered by silver nanoparticles
194
195 91 deposited on two different clays-based materials used as carriers during the digestion. A three-
196
197 92 step enzymatic incubation for the study of the transformations of silver under digestive
198
199 93 conditions was proposed. Total amount of silver released and percentage of ionic silver
200
201 94 (ultrafiltered through a 3 kDa pore size membrane) were determined by ICPMS. Other silver
202
203 95 forms released were characterised by Asymmetric Flow Field-Flow Fractionation (AF4) coupled
204
205 96 to ICPMS as detector, together with UV-Vis and Field Emission Scanning Electronic Microscopy
206
207 97 (FESEM). A second study, an *in vivo* assay with weaned pigs fed with these two materials was
208
209 98 proposed to determine the effect of silver retention in the animal (liver and muscle have been
210
211 99 taken as target organs) and elimination by the faeces, so differences between the two
212
213 100 nanocomposites in the fractions characterised in the *in vitro* assays could be compared to *in vivo*
214
215 101 absorption and excretion values. This is the first time that *in vitro* and *in vivo* results are
216
217 102 compared to establish the relationship between the processes during digestion (*in vitro*) with
218
219 103 the effects on the animal treated (*in vivo* assays) with nanomaterials.
220
221
222
223
224

105 **2. Material and methods**

107 *2.1 Materials*

108 Two different silver nanoparticle-based clays used in animal feed were studied: kaolinite
231
232 109 ($\text{Al}_2\text{Si}_2\text{O}_5(\text{OH})_4$) and sepiolite ($\text{Mg}_4\text{Si}_6\text{O}_{15}(\text{OH})_2 \cdot 6\text{H}_2\text{O}$), both containing silver nanoparticles
233
234
235
236

237
238
239 110 (kaolinite-Ag, sepiolite-Ag) and provided by Laboratorios Enosan, Ltd, Spain. These
240
241 111 nanocomposites were characterised by FESEM where the laminar structure of the kaolinite
242
243 112 microparticles and the fibrous one of the sepiolite were observed (Figure 1). Silver was detected
244
245 113 as spheroidal nanoparticles with average diameters of ca. 30 nm for kaolinite-Ag and ca. 25 nm
246
247 114 for the sepiolite-Ag. The silver content in clays was determined by F-AAS following an acid
248
249 115 digestion, leading to a silver content of 1.07 ± 0.06 % (n=3) (w/w) for kaolinite-Ag and $0.56 \pm$
250
251 116 0.02 % (n=3) (w/w) for sepiolite-Ag.
252
253
254 117
255
256 118

257 119 *2.2 Instrumentation*

260 120 A Perkin-Elmer Sciex model ELAN DRC-e ICP mass spectrometer (Perkin Elmer, Toronto, Canada)
261
262 121 was used throughout. The sample introduction system consisted of a glass concentric Slurry
263
264 122 nebulizer and a baffled cyclonic spray chamber (Glass Expansion, Melbourne, Australia).
265
266 123 Moreover, a flame AAS (F-AAS) AAnalyst 200 (Perkin Elmer, Toronto, Canada) was used for the
267
268 124 determination of total silver content in clays.

270 125 The AF4 system used was an AF2000 (Postnova Analytics, Landsberg, Germany). The trapezoidal
271
272 126 channel was 27.5 cm in length and from 2 to 0.5 cm in width, and the spacer used for all the
273
274 127 measurements was 350 μm thick. An ultrafiltration membrane of polyether sulfone (PES) (cut-
275
276 128 off 5 kDa; Postnova Analytics) was used as the accumulation wall.

278 129 FESEM images were obtained using a Carl Zeiss MERLIN™ (Nano Technology Systems, Jena,
279
280 130 Germany). The microscope was equipped with an energy-dispersive X-ray (EDX) analysis system
281
282 131 INCA 350 (Oxford Instruments, Abingdon, United Kingdom). Before FESEM-EDX analysis,
283
284 132 samples were coated with a carbon layer to enhance conductivity. Carbon coating was
285
286 133 performed with a Leica EM SCD500 (Leica Microsystem, Vienna, Austria) high vacuum sputter
287
288 134 coater.

292 136 *2.3 Reagents*

296
297
298 137 Aqueous silver solutions were prepared from a standard stock solution of 1000 mg L⁻¹ (Panreac,
299
300 138 Barcelona, Spain) by dilution by accurately weighing (\pm 0.1 mg). The carrier used for AF4
301
302 139 separation was prepared dissolving the corresponding mass of sodium dodecylsulphate (SDS)
303
304 140 (BioRad, California, USA) in ultrapure water (Milli-Q Advantage, Molsheim, France). Sodium
305
306 141 dihydrogen phosphate monohydrate (NaH₂PO₄·H₂O) (Sigma Aldrich, St. Louis, EE.UU.); disodium
307
308 142 hydrogen phosphate (Na₂HPO₄) (Sigma Aldrich); hydrochloric acid (Baker Instra Analyzed for
309
310 143 Trace Metals Analysis, J.T. Baker, Holland); pepsin (isolated from pig gastric mucosa, Sigma
311
312 144 Aldrich); sodium hydroxide (NaOH) (Scharlau, Barcelona, Spain); pancreatin (from porcine
313
314 145 pancreas, Sigma Aldrich); ethylenediaminetetraacetic acid (EDTA) (Scharlau) and Viscozyme
315
316 146 (Lysing Enzyme from *Aspergillus* sp., trademark of Novozymes Corp., Sigma Aldrich) were used
317
318 147 in the *in vitro* digestibility assays.
319
320
321
322 148

324 149 *2.4. Analytical procedures*

326 150 *2.4.1. Determination of total silver content from clay nanocomposites*

328 151 100 mg of each material were weighed (\pm 0.1 mg) and HNO₃ (1:1) (J.T. Baker, Holland) was
329
330 152 added, heating and allowing to evaporate near to dryness. The remaining solid was resuspended
331
332 153 in conc. HNO₃ and the solution was made up to 15 mL of 10 % (v/v) HNO₃ in a conical tube. The
333
334 154 suspensions were centrifuged for 10 min at 3000 rpm. The supernatant was removed, and the
335
336 155 solid residue was washed with HNO₃. The supernatant and washing solutions were combined
337
338 156 and made up to 50 mL of 10 % (v/v) HNO₃. Samples were diluted 1:10 with 10 % (v/v) HNO₃ prior
339
340 157 to the F-AAS analysis.
341
342
343
344 158

346 159 *2.4.2. Determination of silver released from clay nanocomposites*

348 160 125 mg of kaolinite-Ag or sepiolite-Ag were put into polyethylene tubes filled with 50 mL of
349
350 161 ultrapure water or HCl 0.01 M (depending on the release assay) and placed in a rotary tumbler

355
356
357 162 for 24 hours in the case of ultrapure water or 2 hours in the case of HCl 0.01 M at 29 rpm and
358
359 163 room temperature in darkness. Then, 10 mL of the suspensions were taken and centrifuged for
360
361 164 10 min and 20°C at 1430 rpm for kaolinite-Ag and at 1808 rpm for sepiolite-Ag (Heraeus
362
363 165 Multifuge X1R, Thermo Fisher Scientific, Waltham, EE.UU.). Centrifugation conditions were set
364
365 166 considering the different density of both materials (kaolinite-Ag: 2.6 g cm⁻³; sepiolite-Ag: 2.0 g
366
367 167 cm⁻³) in order to remove particle sizes larger than 0.5 µm, according to the procedure described
368
369 168 by Bolea et al. [28].
370
371

372 169

373 374 170 *2.4.3. In vivo experimental design and sample collection*

375
376 171 36 male piglets weaned at 25 ± 3 days of age and weighing 7.08 ± 0.03 kg weight were randomly
377
378 172 allocated to three groups (n=6) and housed in 100% slotted floor pens (2.0 x 2.0 m) provided
379
380 173 with a grow feeder and an automatic drinking device, in a temperature-controlled barn (23-
381
382 174 25°C). Procedures were carried out under the Project License PI53/14 approved by the Ethical
383
384 175 and Animal Welfare Committee of the University of Zaragoza, Spain. The care and use of animals
385
386 176 were performed according to the Spanish Policy for Animal Protection RD53/2013, which meets
387
388 177 the European Union Directive 2010/63 on the protection of animals used for experimental and
389
390 178 other scientific purposes. Piglets received a prestarter (first 14 days after weaning) or starter
391
392 179 (from 15 to 35 days after weaning) diets formulated according to their needs. One group of
393
394 180 piglets received the feed not supplemented (control), whereas the other two groups were given
395
396 181 the feed supplemented with either kaolinite-Ag or sepiolite-Ag (20 mg Ag/Kg feed). After that
397
398 182 period, all animals received a common commercial feed from 36 to 62 days after weaning,
399
400 183 resulting, on average, 1.19 kg/d on fresh matter basis. The experimental diets were given *ad*
401
402 184 *libitum*, and pigs had free access to fresh water throughout the experiment.

403
404
405
406 185 On days 14 and 62 of the experiment, 18 pigs (six per treatment on each day) were slaughtered
407
408 186 (average weight of animals at slaughter were 10.1 kg and 35.5 kg respectively) after previous
409
410
411
412
413

414
415
416 187 stunning with CO₂ and after three hours of feed and water deprivation. Representative samples
417
418 188 of liver (on both slaughter days), muscle from the *biceps femoralis* (on 62nd day slaughter) and
419
420 189 rectal content (on 14th day slaughter) were taken, frozen at -20°C and lyophilized for subsequent
421
422 190 Ag analysis to measure tissue retention and faecal excretion.
423
424
425
426 191

427 192 *2.4.4. Determination of silver content of in vivo samples*

429 193 Lyophilized liver, muscle and faeces samples were ground manually to a particle diameter below
430
431 194 1 mm. A ground sample (200 mg) was weighed accurately (± 0.1 mg) in a microwave digestion
432
433 195 vessel. 7 mL of conc. HNO₃ and 3 mL of conc. HCl were added and the digestion was performed
434
435 196 at 200 °C and 800 psi for 30 min. In order to avoid the formation of insoluble AgCl the digestion
436
437 197 was performed in the presence of excess of chloride to stabilize silver as AgCl₃⁻ [29]. After
438
439 198 digestion the volume was made up to 50 mL with 3 % HCl (v/v). Total silver content was then
440
441 199 quantified by ICPMS.
442
443
444
445 200

446 201 *2.4.5. Digestibility assays: in vitro enzymatic incubation*

448 202 The *in vitro* three-step enzymatic incubation procedure described by Boisen *et al.* [30] was
449
450 203 followed. This procedure was designed for estimating protein/dry matter digestibility in pigs. An
451
452 204 amount of 100 mg of kaolinite-Ag or sepiolite-Ag were weighed in 250 mL polypropylene (PP)
453
454 205 Erlenmeyer flasks, to get an initial concentration for each clay in the resultant medium of 2.8 g
455
456 206 L⁻¹ (corresponding to an estimated silver concentration in the digestive system of 28 mg L⁻¹,
457
458 207 according to the fixed dosage in feed of weaned piglets (20 mg Ag/kg feed)). In Step 1, 25 mL of
459
460 208 phosphate buffer (0.1 M, pH 6.0) and 10 mL of 0.2 M HCl were added to each flask in this order,
461
462 209 and pH was adjusted to 2.0; then, 1 mL of a freshly prepared pepsin solution (25 g L⁻¹) was added.
463
464 210 Finally, flasks were closed and put into an incubator (OVAN, Barcelona, Spain) at 39°C and stirred
465
466 211 at 99 rpm for two hours. The Step 2 consisted of the addition to the mixture from Step 1 of 10
467
468 212 mL of a phosphate buffer (0.2 M, pH 6.8) and 5 mL of a 0.6 M NaOH solution. Then the pH was
469
470
471
472

473
474
475 213 adjusted to pH 6.8 and 1 mL of a freshly prepared pancreatin solution (100 g L⁻¹) is added. Flasks
476
477 214 were closed and incubated again under continuous stirring at 99 rpm and 39°C for 4 hours.
478
479 215 Finally, in Step 3 10 mL of a 0.2 M EDTA solution were added to the mixture and the pH was
480
481 216 adjusted to pH 4.8. Finally, 0.5 mL of Viscozyme, a multi-enzyme complex containing cellulases,
482
483 217 were added. Flasks were closed and incubated under the same conditions for 18 hours. All the
484
485 218 flasks were weighed after the addition of the chemicals in each step to know the incubation
486
487 219 volume. The pH adjustments were made with 1 M HCl or 1 M NaOH solutions, depending on the
488
489 220 case. *In vitro* assays with an initial addition of 1 mg L⁻¹ of silver (I) were also performed to check
490
491 221 the recovery of silver during the process. Assays were made in duplicate. At the end of each
492
493 222 step, 10 mL of the suspensions were taken and centrifuged to remove particles larger than 0.5
494
495 223 µm. The viscosity and density of the media were previously measured to adjust the speed of the
496
497 224 centrifuge. Thus, the *in vitro* assays performed with kaolinite-Ag and silver (I) were subjected to
498
499 225 centrifugation for 10 min at 415 x g and 20°C (Heraeus Multifuge X1R, Thermo Fisher Scientific,
500
501 226 Walthman, EE.UU.); whereas those with sepiolite-Ag were centrifuged at 666 x g. Samples were
502
503 227 diluted with 5 % HCl (v/v) prior to the quantification by ICPMS.
504
505
506
507 228
508
509 229 *2.4.6. Determination of dissolved silver fraction by ultrafiltration*
510
511 230 The dissolved silver fraction was isolated by using Nanosep centrifugal ultrafilter devices (Pall,
512
513 231 Ann Arbor, EE.UU.) with cut-off membranes of 3 kDa (estimated to be equivalent to a 2 nm
514
515 232 hydrodynamic diameter). Before used, ultrafilter devices were washed twice by centrifugation
516
517 233 with 500 µL of ultrapure water. The second wash solution was used to check for any potential
518
519 234 contamination. Suspensions from *in vitro* assays previously centrifuged were sonicated for two
520
521 235 minutes; and a volume of 500 µL were subjected to centrifugation for 20 min at 9056 x g and
522
523 236 20°C (Heraeus Multifuge X1R, Thermo Fisher Scientific, Walthman, EE.UU.). The ultrafiltered
524
525 237 fraction (ca. 500 µL) was diluted up to 5 mL with 5 % HCl (v/v) prior to ICPMS analysis.
526
527
528
529
530
531

532
533
534
535
536
537
538
539
540
541
542
543
544
545
546
547
548
549
550
551
552
553
554
555
556
557
558
559
560
561
562
563
564
565
566
567
568
569
570
571
572
573
574
575
576
577
578
579
580
581
582
583
584
585
586
587
588
589
590

238

239 *2.4.7. Detection of different silver forms by Asymmetrical Flow Field Flow Fractionation (AF4).*

240 100 μL of the *in vitro* suspensions and 50 μL of the silver release suspensions in water

241 (centrifuged fractions $< 0.5 \mu\text{m}$) were directly injected in the AF4 channel. A 0.01 % (m/v) SDS

242 solution prepared in ultrapure water and adjusted to pH 8 was used as the carrier. Two different

243 crossflow programs, listed in Table 1, were used. The carrier was degassed prior to use by an

244 online vacuum degasser. The eluent was directed from the channel through an UV-Vis diode-

245 array detector (Shimadzu, Duisburg, Germany) recording the absorbance signal in the range

246 from 200 to 650 nm and to the ICPMS spectrometer, used as a silver specific detector.

247 *2.5. Statistical analysis*

248 To make a comparison between the variations of silver content in liver and faeces of pigs fed

249 with the two nanocomposites used along this work (sepiolite-Ag and kaolinite-Ag) and the

250 control, a one-way analysis of variance (ANOVA) was applied. Microsoft Excel version Office 365

251 (Microsoft Corp., KY, USA) was used to conduct statistical analysis. Values were expressed as

252 mean and standard deviation. Remarkable variations were detected at the $p < 0.05$ significance

253 level.

254

255 **3. Results and discussion**

256 *3.1. Characterisation of the clay nanocomposites. Mobilisation of silver from nanocomposites in*

257 *ultrapure water*

258 The mobilisation of silver from the two clays materials was studied firstly in ultrapure water,

259 following the procedure described in section 2.4.2 and 2.4.6. The percentage of silver in the

260 leachates with respect to the total amount in the composite was similar in both cases (between

261 40-48%) as shown in Table 2. However, a large difference was observed when comparing the

262 forms of silver in solution. In the case of kaolinite-Ag, most of the silver mobilised ($91 \pm 5 \%$) was

591
592
593 263 found in the ultrafiltrate (fraction with a molecular weight < 3 kDa), which likely corresponds to
594
595 264 ionic silver. In comparison, the lower percentage of silver found in the ultrafiltrate of the
596
597 265 sepiolite-Ag assay suggests that a significant fraction of silver is mobilised as AgNPs or associated
598
599 266 to small particles of sepiolite remaining in solution. This fact could be explained by its higher
600
601 267 sorption capacity [31], which may reduce the amount of ionic silver in solution, together with
602
603 268 the less effective centrifugation of the sepiolite, caused by its laminar structure, resulting in a
604
605 269 large percentage of silver associated to microparticles of sepiolite retained in the ultrafilter.
606
607
608
609 270

610 271 *3.2. Behaviour of silver during in vitro digestion processes. Quantification of silver released.*

612 272 The potential transformations of AgNPs during digestion is a complex and dynamic process, and
613
614 273 the occurrence of agglomeration/aggregation and dissolution should be considered. Hence, a
615
616 274 study about the release of silver in an *in vitro* digestibility assay was performed to know the
617
618 275 behaviour of the silver-based nanocomposites in each step of the digestion process. It consists
619
620 276 of a three-step enzymatic incubation, as a simulation of gastric (Step 1), small intestine (Step 2)
621
622 277 and the large intestine (Step 3) digestion processes. As a first approach, the silver mobilised from
623
624 278 the two materials kaolinite-Ag and sepiolite-Ag (described in section 2.1) was quantified by
625
626 279 ICPMS, as described in section 2.4.5. Table 3 shows the percentage of silver mobilised in each
627
628 280 step of the assay with respect to the total amount of silver in the nanocomposites.
629
630
631
632 281

633
634 282 Different behaviours between the two additives and between the different steps of the digestive
635
636 283 process were observed. Regardless of the composite studied, a low mobilisation of silver in Step
637
638 284 1 was obtained. These percentages of silver released during Step 1 are in good agreement with
639
640 285 those obtained when the composites were subjected to a simple simulation of acidic medium in
641
642 286 stomach with 0.01 M HCl for 2 hours. (0.9 ± 0.2 % for kaolinite-Ag and 1.2 ± 0.3 % for sepiolite-
643
644 287 Ag). Additionally, the formation of AgCl on both clay surfaces was observed by FESEM (Figures
645
646
647
648
649

650
651
652 288 S1 and S2 Electronic supplementary information), which may also justify the low values obtained
653
654 289 of silver mobilised during Step 1.
655
656 290
657 291 It should be bear in mind that low silver recoveries ($51.2 \pm 0.5\%$, which represents the percentage
658
659 292 of silver determined respect to the silver added) were also obtained in Step 1 when silver was
660
661 293 added as AgNO_3 , where the presence of chlorides in the medium can contribute to the formation
662
663 294 of AgCl precipitate that might be lost during centrifugation. On the contrary, recoveries close to
664
665 295 100% for AgNO_3 were obtained in Steps 2 and 3.
666
667 296 The larger amount of silver mobilised during Steps 2 and 3 observed with both materials could
668
669 297 be related to oxidation processes from AgNPs on clays surface or alternatively, the solubilization
670
671 298 of AgCl precipitated during Step 1, caused by the addition of enzymes and complexing agents
672
673 299 during these steps, being higher with kaolinite-Ag, particularly in Step 2. In any case, the
674
675 300 percentages of silver released along these three steps are much lower than the silver mobilised
676
677 301 in ultrapure water. This is relevant since comparatively, only a small fraction of the silver is
678
679 302 mobilised during the simulated digestion process, which could have a consequence on its
680
681 303 bioaccessibility.
682
683
684
685
686

687 306 *3.3 Study of silver species and their evolution during the in vitro digestion processes.*

688
689 307 The fraction of silver mobilised could be composed of ionic silver, silver (I) complexes with those
690
691 308 species present in the media (enzymes mostly), silver nanoparticles and precipitate silver(I) salts,
692
693 309 as well as silver associated to clay microparticles remaining in suspension after centrifugation
694
695 310 (sizes smaller than $0.5 \mu\text{m}$). Ultrafiltration using a 3 kDa membrane pore size was employed to
696
697 311 separate and quantify the fraction constituted by both free silver ions and silver complexes with
698
699 312 low molecular weight substances ($< 3 \text{ kDa}$). Results, expressed as percentage of silver
700
701 313 ultrafiltered respect to the total silver content, are shown in Table 3. All these values are
702
703 314 relatively low ($< 4\%$), being larger in the case of Step 3 respect to Step 2 and 1. Bove et al [22]
704
705
706
707
708

709
710
711 315 also reported low percentages of silver in ultrafiltrates at 3 kDa in the *in vitro* human digestion
712
713 316 simulation in the small intestine medium, although they used a reference material NM300k
714
715 317 (from the Join Research Centre (JRC), which contains AgNPs of about 15 nm size) for their
716
717 318 studies.

719 319 To obtain more information about all the species of silver > 3 kDa along the *in vitro* digestion,
720
721 320 the suspensions (fraction < 0.5 μm) were analysed directly by AF4-UV-Vis-ICPMS under the
722
723 321 conditions described in Section 2.4.7. Flow Field-flow fractionation is a size-based separation
724
725 322 technique where separation takes place in a channel without a stationary phase, caused by the
726
727 323 action of a crossflow applied perpendicularly to a laminar flow, so small particles elute first in
728
729 324 normal mode. The basis of separation and a detailed description of theory can be found in [32].
730
731 325 Program A (see Table 1), optimized for AgNPs size characterisation [33] was used, and the
732
733 326 fractograms corresponding to leachates of both nanocomposites are shown in Figure 2. Step 1
734
735 327 (stomach simulation) was not measured given the low percentage of silver solubilized and the
736
737 328 low silver recoveries found. Fractograms from kaolinite-Ag showed two non-resolved
738
739 329 distributions in Steps 2 and 3, whereas only one peak was observed in the fractograms from
740
741 330 sepiolite-Ag. The first distribution in the kaolinite-Ag fractograms could be related to a fraction
742
743 331 of silver associated to enzymes present in the media, which would be in good agreement with
744
745 332 the absorbance at 280 nm observed, typical of organic matter. Also a recovery assay by addition
746
747 333 of AgNO_3 to media from step 2 and 3 was made, quantifying the percentage of silver found in
748
749 334 the < 3 kDa fraction by ultrafiltration. In step 2, a recovery value as low as $22 \pm 3 \%$ was obtained,
750
751 335 whereas this value increased up to $67 \pm 5 \%$ during step 3. These results suggest that in step 2
752
753 336 silver (I) is likely associated in a large extent to enzymes (which are retained in the ultrafiltrate),
754
755 337 whereas in step 3 most of the silver (I) pass through the filter, likely as EDTA complex, not being
756
757 338 retained. Moreover, if these fractograms (Fig. 2 a-b) are compared to the ones obtained for a
758
759 339 suspension of kaolinite-Ag in ultrapure water for 24 hours (Figure S3 - Electronic supplementary
760
761 340 information), just a signal related to the second distribution is detected, confirming the organic
762
763
764
765
766
767

768
769
770 341 nature of the first silver signal in the digestive media (not present in ultrapure water assay). The
771
772 342 lower amount of silver in the sepiolite-Ag media and its sorption capacity [31] could justify the
773
774 343 absence of this fraction in the corresponding fractograms.
775

776
777 344 Suspensions from Steps 2 and 3 of the kaolinite-Ag assays were injected following the crossflow
778
779 345 program B (Table 1). This program applied a higher constant crossflow at the beginning to
780
781 346 increase the resolution on the separation of the first fraction followed by a linear decay to elute
782
783 347 the rest of species injected. Figure 3 shows the corresponding fractograms for kaolinite-Ag under
784
785 348 these conditions. As expected, a slight improvement on the resolution of the first fraction was
786
787 349 obtained (up to three peaks not resolved are observed in Step 2 fractogram, which corresponds
788
789 350 to different forms of silver). In Step 2 fractogram (Fig. 3 a), there is no correspondence between
790
791 351 the silver signal and absorbance at 280 nm. Apparently, most of the organic fraction is eluted at
792
793 352 the beginning of the fractogram, coeluting with the void peak, whereas the silver is eluted later,
794
795 353 showing correspondence with the small shoulder observed at 7 min of the 280 nm absorbance
796
797 354 signal. In the case of Step 3, there is coincidence between the maxima of both signals (silver and
798
799 355 absorbance at 280 nm), with a peak at 6.4 min, and a peak and a shoulder in the case of UV-Vs
800
801 356 signal at 8.0 min. The presence of viscozyme (an enzyme complex containing a wide range of
802
803 357 carbohydrases, including arabanase, cellulase, β -glucanase, hemicellulase, and xylanase) in
804
805 358 addition to the enzymes from Steps 1 and 2, justify the larger absorbance signal and the silver
806
807 359 associated to these species. Therefore, it can be stated that a large fraction of silver released
808
809 360 from kaolinite-Ag as Ag(I) would be associated to the enzymatic digestion processes that take
810
811 361 place through the digestive tract.
812
813

814
815 362
816
817
818 363 With respect to the second distribution, it could correspond to larger size species according to
819
820 364 the elution time, such as silver nanoparticles, although no UV-Vis absorption signal at ca. 400
821
822 365 nm (due to the plasmon resonance of silver nanoparticles) was observed in any case.
823
824
825
826

827
828
829 366 Alternatively, it is possible that silver forms insoluble species (such as chlorides) inside the
830
831 367 channel. In fact, some studies carried out with AgNPs in an *in vitro* human gastrointestinal
832
833 368 digestion model [18] showed the presence of big clusters of 0.2-0.5 μm with chlorine in their
834
835 369 composition as revealed by EDX analysis. Kejlova et al. [20] also studied the changes on size and
836
837 370 morphology of AgNPs subjected to action of simulated saliva, gastric and intestinal fluids. The
838
839 371 authors stated that AgNPs agglomerate and partially react to form AgCl during exposure to
840
841 372 gastric fluids, and strong coagulation occurred when AgNPs were mixed with the simulated
842
843 373 intestinal fluid supplemented with pancreatin. They concluded that all these changes depended
844
845 374 on pH, ionic strength and the presence of proteins in these fluids.
846
847
848

849 375 In this case, this silver fraction could be the consequence of an artefact of the technique and
850
851 376 formed during the separation process. The collection of this fraction and subsequent analysis by
852
853 377 FESEM did not give any further information about its nature, probably due to the low
854
855 378 concentration obtained after the separation by AF4. However, this is not something particular
856
857 379 of this technique, and other techniques reported in bibliography [34], like DLS, Electronic
858
859 380 Microscopy or Single Particle-ICPMS, can also lead to wrong conclusions in such complex media.
860
861 381 Besides, differences on the conditions used in the *in vitro* assays described in literature, such as
862
863 382 salt content, pH used, presence of different enzymes, or nanoparticles concentration make
864
865 383 comparison between results even more difficult.
866
867
868

868 384

870 385 *3.4. Effect of composite nature on silver retained and excreted from in vivo assays*

871

872 386 Total silver content in liver and muscle tissues and faeces from animals fed with a diet
873
874 387 supplemented with kaolinite-Ag and sepiolite-Ag were determined as described in Section 2.4.4.
875
876 388 Average results from the analysis are shown in Table 4. According to these results it can be stated
877
878 389 that silver is significantly accumulated in liver in the period when pigs are fed with
879
880 390 nanocomposites, compared to control. Also, the kaolinite-Ag provides a higher amount of silver
881
882
883
884
885

886
887
888 391 retained than the sepiolite-Ag, although differences cannot be considered significant ($P>0.05$ (at
889
890 392 14 days of the beginning of the assay; P values are given in Table 4, comparing values between
891
892 393 the materials and treatment days). On the other hand, a decrease in the silver content in the
893
894 394 liver of animals subjected to a second diet without silver for four weeks was observed.
895
896 395 Differences were significant for kaolinite-Ag ($P<0.05$ when compare results from day 14 to day
897
898 396 62), but not in the case of sepiolite-Ag ($P>0.05$). Previous results [12] showed similar levels of
899
900 397 silver retention (1.35 and 2.45 $\mu\text{g Ag/g}$) in the liver tissue of pigs feed with a diet supplemented
901
902 398 with 20 or 40 mg of metallic silver as NPs/kg feed for 35 days after weaning respectively.
903
904
905 399
906 400 Determination of total silver content in faeces showed that, although silver was detected in the
907
908 401 faeces of control animals, these levels were much lower than those observed for pigs treated
909
910 402 with silver and could be attributed to some level of cross-contamination. Moreover, the levels
911
912 403 of silver excreted were especially high compared to those retained in the liver tissues. No
913
914 404 significant differences were observed in the silver content of faeces depending on the additive
915
916 405 used ($P>0.05$), although these values were higher in the case of sepiolite-Ag considering the
917
918 406 average value.
919
920 407 Attending to all these results, a tendency between the *in vitro* results and the silver retained in
921
922 408 liver and excreted can be established. Thus, the lower amount of silver detected in the intestinal
923
924 409 simulation steps for sepiolite-Ag nanocomposite respect to the kaolinite-Ag levels is also
925
926 410 reflected on a lower amount of silver accumulated in liver, as shown by the results from *in vivo*
927
928 411 assays on average. In the same way, given the larger proportion of silver released from kaolinite-
929
930 412 Ag during the *in vitro* assays, the amount of silver excreted is consequently lower regarding the
931
932 413 levels quantified for sepiolite-Ag. However, they should be considered as a first approach since
933
934 414 no statistical differences were found when comparing both materials in the *in vivo* assays, so
935
936 415 further studies will be needed to confirm these findings. Finally, silver levels in muscle were
937
938 416 determined at the end of the experiment (after 62 days) to evaluate the potential ingestion of
939
940
941
942
943
944

945
946
947 417 silver through the consumption of meat from pigs treated with these nanocomposites. Neither
948
949 418 in control nor in kaolinite-Ag or sepiolite-Ag significant concentrations were detected (values
950
951 419 under the limit of detection ($0.009 \mu\text{g Ag g}^{-1}$) were obtained) so silver in muscles were in the
952
953 420 same order that those found in control experiments.
954

955 421
956 422

958 423 **4. Conclusions**

959 424 According to the assays carried out, it can be concluded that the materials used as supports for
960
961 425 silver nanoparticles, which are used as additives in animal feed (kaolinite and sepiolite) show
962
963 426 differences with respect to the silver mobilised and its forms. There is no evidence about a
964
965 427 significant release of silver nanoparticles from any of these two materials along the *in vitro*
966
967 428 digestibility assay, in any of the three steps. The formation of silver chloride seemed to be the
968
969 429 dominant process during the Step 1 (stomach simulation), which limited the release of silver to
970
971 430 the medium. The analysis of the media from intestine simulation Steps (2 and 3) by AF4-UV-Vis-
972
973 431 ICPMS allowed to confirm that silver released forms complexes in a large extent with those
974
975 432 species present in the medium (enzymes mostly) in the case of kaolinite-Ag. This fraction was
976
977 433 not present when sepiolite-Ag was used, likely due to its fibrous structure and sorption capacity.
978
979 434 The presence of another form of silver was detected in both intestine simulation steps and with
980
981 435 the two materials tested. This fraction would correspond to insoluble silver forms, although their
982
983 436 presence in the original medium was not proved, which shows some of the limitations of the
984
985 437 techniques used when applied to such complex systems.
986
987
988
989

990 438 Along this study, a tendency between the *in vitro* results and the silver retained in liver and
991
992 439 excreted in the *in vivo* assays with weaned pigs supplemented with the silver-based
993
994 440 nanocomposites was found. The absence of silver at significant values in muscle tissues makes
995
996 441 this technology a potential alternative as growth promoter, although the environmental impact
997
998
999

1004
1005
1006 442 of faeces should be evaluated, given the silver content found that would limit its land application
1007
1008 443 as manure management practice.
1009
1010
1011 444
1012
1013
1014 445 **Acknowledgments**
1015
1016
1017 446 This work was supported by the Spanish Ministry of Economy and Competitiveness and the
1018
1019 447 European Regional Development Fund [project CTQ2015-68094-C2-1-R (MINECO/FEDER)] and
1020
1021 448 Gobierno de Aragón (project E29_17R) and FEDER 2014-2020 "Construyendo Europa desde
1022
1023 449 Aragón". The authors would like to acknowledge the use of Servicio General de Apoyo a la
1024
1025 450 Investigación-SAI, Universidad de Zaragoza, for ICPMS measurements and Laboratorios Enosan
1026
1027 451 S.L. for providing the nanomaterials used along this work.
1028
1029
1030
1031
1032
1033
1034
1035
1036
1037
1038
1039
1040
1041
1042
1043
1044
1045
1046
1047
1048
1049
1050
1051
1052
1053
1054
1055
1056
1057
1058
1059
1060
1061
1062

1063
1064
1065
1066
1067
1068
1069
1070
1071
1072
1073
1074
1075
1076
1077
1078
1079
1080
1081
1082
1083
1084
1085
1086
1087
1088
1089
1090
1091
1092
1093
1094
1095
1096
1097
1098
1099
1100
1101
1102
1103
1104
1105
1106
1107
1108
1109
1110
1111
1112
1113
1114
1115
1116
1117
1118
1119
1120
1121

452 **REFERENCES**

453 [1] Regulation (EC) N° 1831/2003 of the European Parliament and of the Council of 22
454 September 2003 on additives for use in animal nutrition, Off. J. Eur. Union. (2003)
455 L268/29.

456 [2] L.D. Franco, M. Fondevila, M.B. Lobera, C. Castrillo, Effect of combinations of organic
457 acids in weaned pig diets on microbial species, *J. Anim. Physiol. Anim. Nutr. (Berl)*. 89
458 (2005) 88–93.

459 [3] J.P. Griggs, J.P. Jacob, Alternatives to antibiotics for organic poultry production, *J. Appl.*
460 *Poult. Res.* 14 (2005) 750–756. doi:10.1093/japr/14.4.750.

461 [4] M. Murphy Cowan, Plant Products as Antimicrobial agents, *Clin. Microbiol. Rev.* 12
462 (1999) 564–582. doi:10.1016/j.tibtech.2009.09.002.

463 [5] C.-N. Lok, C.-M. Ho, R. Chen, Q.-Y. He, W.-Y. Yu, H. Sun, P.K.-H. Tam, J.-F. Chiu, C.-M.
464 Che, Silver nanoparticles: partial oxidation and antibacterial activities., *J. Biol. Inorg.*
465 *Chem.* 12 (2007) 527–534. doi:10.1007/s00775-007-0208-z.

466 [6] S.P. Deshmukh, S.M. Patil, S.B. Mullani, S.D. Delekar, Silver nanoparticles as an effective
467 disinfectant: A review, *Mater. Sci. Eng. C.* 97 (2019) 954–965.
468 doi:10.1016/j.msec.2018.12.102.

469 [7] B.S. Atiyeh, M. Costagliola, S.N. Hayek, S.A. Dibo, Effect of silver on burn wound
470 infection control and healing: Review of the literature, *Burns.* 33 (2007) 139–148.
471 doi:10.1016/j.burns.2006.06.010.

472 [8] T.C. Dakal, A. Kumar, R.S. Majumdar, V. Yadav, Mechanistic basis of antimicrobial
473 actions of silver nanoparticles, *Front. Microbiol.* 7 (2016) 1–17.
474 doi:10.3389/fmicb.2016.01831.

475 [9] O. Choi, K.K. Deng, N.J. Kim, L. Ross, R.Y. Surampalli, Z. Hu, The inhibitory effects of
476 silver nanoparticles, silver ions, and silver chloride colloids on microbial growth, *Water*
477 *Res.* 42 (2008) 3066–3074. doi:10.1016/j.watres.2008.02.021.

478 [10] E. Sawosz, M. Binek, M. Grodzik, M. Zielinska, P. Sysa, M. Szmidt, T. Niemiec, A.
479 Chwalibog, Influence of hydrocolloidal silver nanoparticles on gastrointestinal
480 microflora and morphology of enterocytes of quails, *Arch. Anim. Nutr.* 61 (2007) 444–
481 451. doi:10.1080/17450390701664314.

482 [11] L. Pineda, A. Chwalibog, E. Sawosz, C. Lauridsen, R. Engberg, J. Elnif, A. Hotowy, F.
483 Sawosz, Y. Gao, A. Ali, H.S. Moghaddam, Effect of silver nanoparticles on growth
484 performance, metabolism and microbial profile of broiler chickens, *Arch. Anim. Nutr.* 66
485 (2012) 416–429. doi:10.1080/1745039X.2012.710081.

486 [12] M. Fondevila, R. Herrer, M.C. Casallas, L. Abecia, J.J. Duchá, Silver nanoparticles as a
487 potential antimicrobial additive for weaned pigs, *Anim. Feed Sci. Technol.* 150 (2009)
488 259–269. doi:10.1016/j.anifeedsci.2008.09.003.

489 [13] I. Sondi, B. Salopek-Sondi, Silver nanoparticles as antimicrobial agent: A case study on *E.*
490 *coli* as a model for Gram-negative bacteria, *J. Colloid Interface Sci.* 275 (2004) 177–182.
491 doi:10.1016/j.jcis.2004.02.012.

492 [14] G. Bergaya, F.; Lagaly, General introduction: clays, clay minerals and clay science.

1122
1123
1124 493 Development in Clay Science, Elsevier The Netherlands, 2013.
1125

1126 494 [15] W.J. Chen, L.C. Hsiao, K.K.Y. Chen, Metal desorption from copper(II)/nickel(II)-spiked
1127 495 kaolin as a soil component using plant-derived saponin biosurfactant, *Process Biochem.*
1128 496 43 (2008) 488–498. doi:10.1016/j.procbio.2007.11.017.

1129
1130 497 [16] S.P. Singh, L.Q. Ma, W.G. Harris, Heavy metal interactions with phosphatic clay:
1131 498 sorption and desorption behavior, *J. Environ. Qual.* 30 (2001) 1961–1968.
1132 499 doi:10.2134/jeq2001.1961.

1133
1134 500 [17] G.S. Martynkova, M. Valaskova, Antimicrobial Nanocomposites Based on Natural
1135 501 Modified Materials: A Review of Carbons and Clays, *J. Nanosci. Nanotechnol.* 14 (2014)
1136 502 673–693. doi:10.1166/jnn.2014.8903.

1137
1138 503 [18] A.P. Walczak, R. Fokkink, R. Peters, P. Tromp, Z.E. Herrera Rivera, I.M.C.M. Rietjens,
1139 504 P.J.M. Hendriksen, H. Bouwmeester, Behaviour of silver nanoparticles and silver ions in
1140 505 an in vitro human gastrointestinal digestion model, *Nanotoxicology.* (2012) 1–13.
1141 506 doi:10.3109/17435390.2012.726382.

1142
1143 507 [19] K. Ramos, L. Ramos, M.M. Gómez-Gómez, Simultaneous characterisation of silver
1144 508 nanoparticles and determination of dissolved silver in chicken meat subjected to in
1145 509 vitro human gastrointestinal digestion using single particle inductively coupled plasma
1146 510 mass spectrometry, *Food Chem.* 221 (2017) 822–828.
1147 511 doi:10.1016/j.foodchem.2016.11.091.

1148
1149 512 [20] K. Kejlová, M. Dvorakova, L. Pindakova, D. Krsek, D. Jírová, L. Kasparova, Behaviour of
1150 513 silver nanoparticles in simulated saliva and gastrointestinal fluid, *Int. J. Pharm.* 527
1151 514 (2017) 12–20. doi:10.1016/j.ijpharm.2017.05.026.

1152
1153 515 [21] C. Kästner, D. Lichtenstein, A. Lampen, A.F. Thünemann, Monitoring the fate of small
1154 516 silver nanoparticles during artificial digestion, *Colloids Surfaces A Physicochem. Eng.*
1155 517 *Asp.* 526 (2017) 76–81. doi:10.1016/j.colsurfa.2016.08.013.

1156
1157 518 [22] P. Bove, M.A. Malvindi, S.S. Kote, R. Bertorelli, M. Summa, S. Sabella, Dissolution test
1158 519 for risk assessment of nanoparticles: a pilot study, *Nanoscale.* 9 (2017) 6315–6326.
1159 520 doi:10.1039/C6NR08131B.

1160
1161 521 [23] I. Gil-Sánchez, M. Monge, B. Miralles, G. Armentia, C. Cueva, J. Crespo, J.M. López de
1162 522 Luzuriaga, M.E. Olmos, B. Bartolomé, D. González de Llano, M.V. Moreno-Arribas, Some
1163 523 new findings on the potential use of biocompatible silver nanoparticles in winemaking,
1164 524 *Innov. Food Sci. Emerg. Technol.* 51 (2019) 64–72. doi:10.1016/j.ifset.2018.04.017.

1165
1166 525 [24] Z. Zhang, R. Zhang, H. Xiao, K. Bhattacharya, D. Bitounis, P. Demokritou, D.J.
1167 526 McClements, Development of a standardized food model for studying the impact of
1168 527 food matrix effects on the gastrointestinal fate and toxicity of ingested nanomaterials,
1169 528 *NanoImpact.* 13 (2019) 13–25. doi:10.1016/j.impact.2018.11.002.

1170
1171 529 [25] W. Wu, R. Zhang, D.J. McClements, B. Chefetz, T. Polubesova, B. Xing, Transformation
1172 530 and Speciation Analysis of Silver Nanoparticles of Dietary Supplement in Simulated
1173 531 Human Gastrointestinal Tract, *Environ. Sci. Technol.* 52 (2018) 8792–8800.
1174 532 doi:10.1021/acs.est.8b01393.

1175
1176 533 [26] L. Böhmert, M. Girod, U. Hansen, R. Maul, P. Knappe, B. Niemann, S.M. Weidner, A.F.
1177 534 Thünemann, A. Lampen, Analytically monitored digestion of silver nanoparticles and
1178 535 their toxicity on human intestinal cells, *Nanotoxicology.* 8 (2014) 631–642.

1181
1182
1183 536 doi:10.3109/17435390.2013.815284.
1184
1185 537 [27] J. Liu, Z. Wang, F.D. Liu, A.B. Kane, R.H. Hurt, Chemical transformations of nanosilver in
1186 538 biological environments, *ACS Nano*. 6 (2012) 9887–9899. doi:10.1021/nn303449n.
1187
1188 539 [28] E. Bolea, F. Laborda, J.R. Castillo, Metal associations to microparticles, nanocolloids and
1189 540 macromolecules in compost leachates: Size characterization by asymmetrical flow field-
1190 541 flow fractionation coupled to ICP-MS, *Anal. Chim. Acta*. 661 (2010) 206–214.
1191 542 doi:10.1016/j.aca.2009.12.021.
1192
1193 543 [29] M. Marchioni, P.H. Jouneau, M. Chevallet, I. Michaud-Soret, A. Deniaud, Silver
1194 544 nanoparticle fate in mammals: Bridging in vitro and in vivo studies, *Coord. Chem. Rev.*
1195 545 364 (2018) 118–136. doi:10.1016/j.ccr.2018.03.008.
1196
1197 546 [30] S. Boisen, J.A. Fernández, Prediction of the total tract digestibility of energy in
1198 547 feedstuffs and pig diets by in vitro analyses, *Anim. Feed Sci. Technol.* 68 (1997) 277–
1199 548 286. doi:10.1016/S0377-8401(97)00058-8.
1200
1201 549 [31] Y. Turhan, P. Turan, M. Doğan, M. Alkan, H. Namli, Ö. Demirbaş, Characterization and
1202 550 adsorption properties of chemically modified sepiolite, *Ind. Eng. Chem. Res.* 47 (2008)
1203 551 1883–1895. doi:10.1021/ie070506r.
1204
1205 552 [32] M. Schimpf, K. Caldwell, J.C. Giddings, eds., *Field-Flow Fractionation Handbook*, John
1206 553 Wiley & Sons, Inc., 2000.
1207
1208 554 [33] E. Bolea, J. Jiménez-Lamana, F. Laborda, J.R. Castillo, Size characterization and
1209 555 quantification of silver nanoparticles by asymmetric flow field-flow fractionation
1210 556 coupled with inductively coupled plasma mass spectrometry, *Anal. Bioanal. Chem.* 401
1211 557 (2011). doi:10.1007/s00216-011-5201-2.
1212
1213 558 [34] F. Laborda, E. Bolea, G. Cepriá, M.T. Gómez, M.S. Jiménez, J. Pérez-Arantegui, J.R.
1214 559 Castillo, Detection, characterization and quantification of inorganic engineered
1215 560 nanomaterials: A review of techniques and methodological approaches for the analysis
1216 561 of complex samples, *Anal. Chim. Acta*. 904 (2016). doi:10.1016/j.aca.2015.11.008.
1217 562
1218
1219 563
1220
1221 564
1222
1223
1224
1225
1226
1227
1228
1229
1230
1231
1232
1233
1234
1235
1236
1237
1238
1239

1240
1241
1242
1243
1244
1245
1246
1247
1248
1249
1250
1251
1252
1253
1254
1255
1256
1257
1258
1259
1260
1261
1262
1263
1264
1265
1266
1267
1268
1269
1270
1271
1272
1273
1274
1275
1276
1277
1278
1279
1280
1281
1282
1283
1284
1285
1286
1287
1288
1289
1290
1291
1292
1293
1294
1295
1296
1297
1298

565 **List of captions**

566

567 **Figure 1.** Kaolinite-Ag: a) Microparticle of kaolinite-Ag with silver nanoparticles on the surface
568 (x8870). b) Magnified micrograph from inset in a) (x20380). c) Magnified micrograph from inset
569 in (b) showing silver nanoparticles on the surface of kaolin sheets (x66000). d) EDX spectra from
570 areas containing silver nanoparticles. Silver was found as spheroidal nanoparticles. Sepiolite-Ag:
571 a) Microparticle of sepiolite-Ag with AgNPs on the surface (x2210). b) Surface of a sepiolite
572 microparticle (x47390). (c) Magnified micrograph from inset in b) (x103360) with backscattered
573 electrons. d) EDX spectra from areas containing silver nanoparticles. Silver was found as white
574 spots.

575

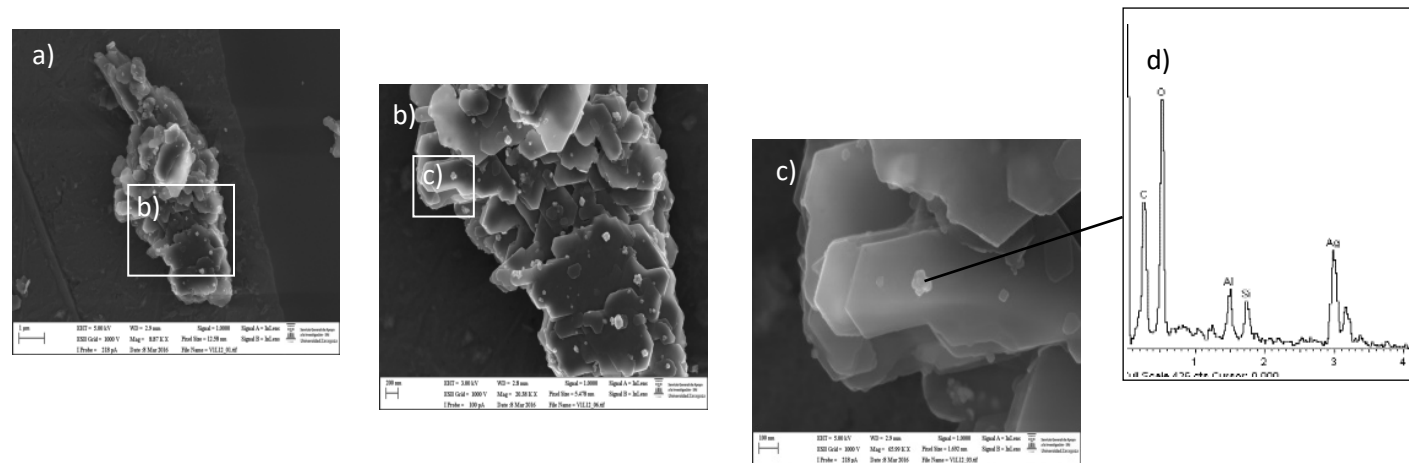
576 **Figure 2** AF4-UV-Vis-ICPMS fractograms of the suspensions from Step 2 (a, c) and Step 3 (b, d)
577 from *in vitro* digestion processes with kaolinite-Ag (a, b) and sepiolite-Ag (c, d). ¹⁰⁷Ag ICPMS
578 signal (black line), absorbance at 280 nm (blue line) and at 405 nm (red line). Crossflow program
579 A (green line).

580 **Figure 3** AF4-UV-Vis-ICPMS fractograms of the suspensions from Step 2 (a) and Step 3 (b) from
581 *in vitro* digestion process with kaolinite-Ag. Magnification of fractograms in right upper corner.
582 ¹⁰⁷Ag ICPMS signal (black line), absorbance at 280 nm (blue line) and at 405 nm (red line).
583 Crossflow program B (green line).

584

Figure 1

Kaolinite-Ag



Sepiolite-Ag

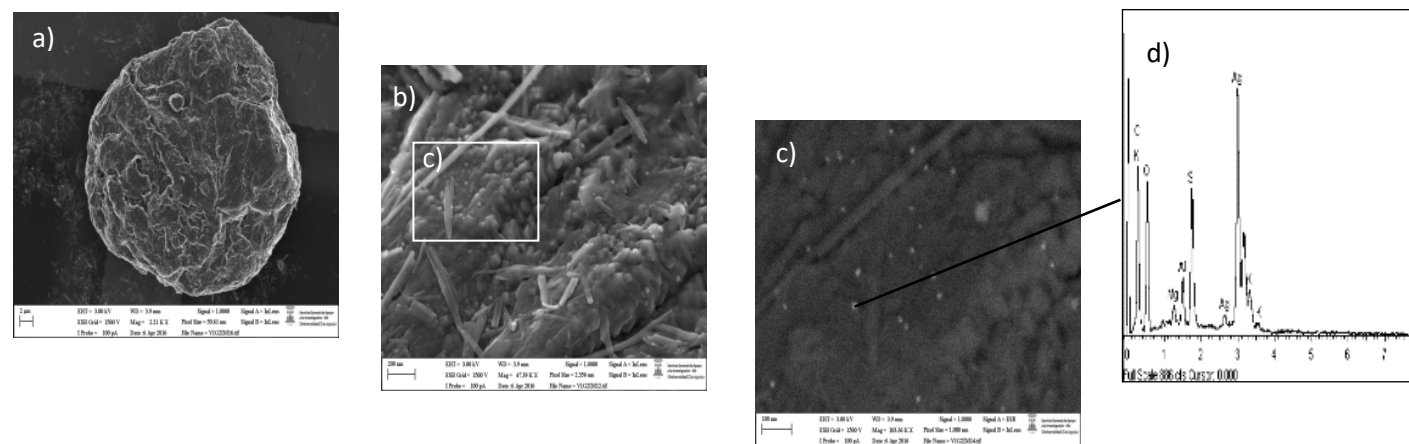
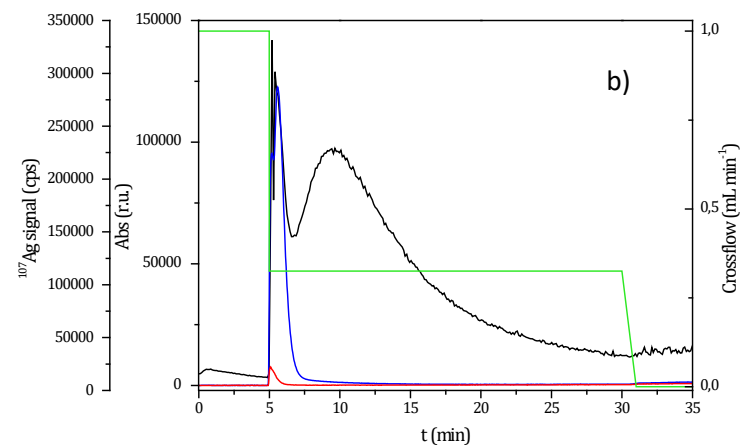
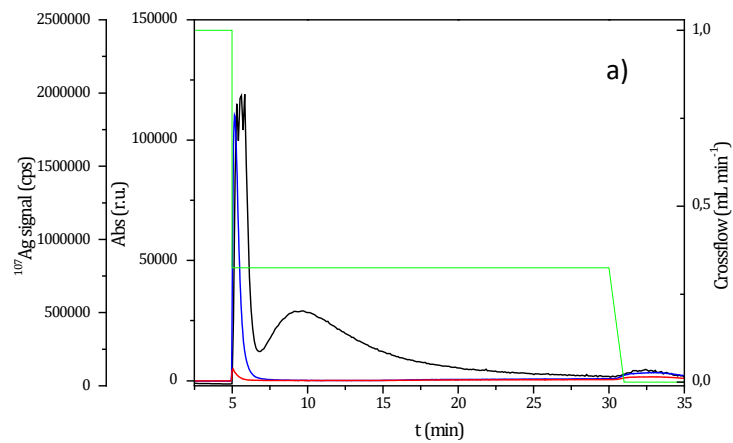


Figure 2

Step 2

Step 3

Kaolinite-Ag



Sepiolite-Ag

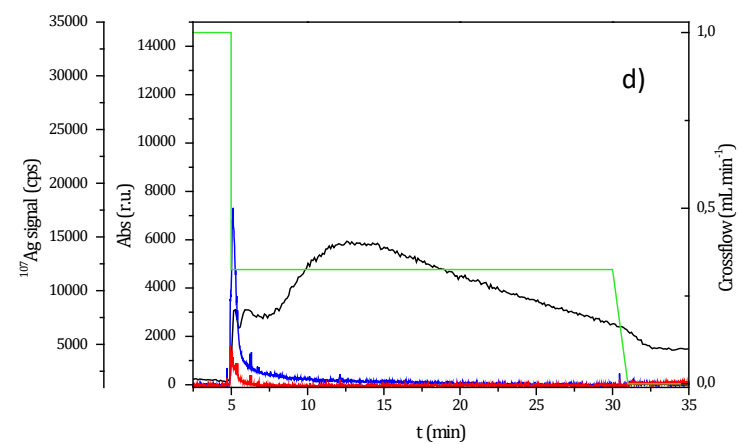
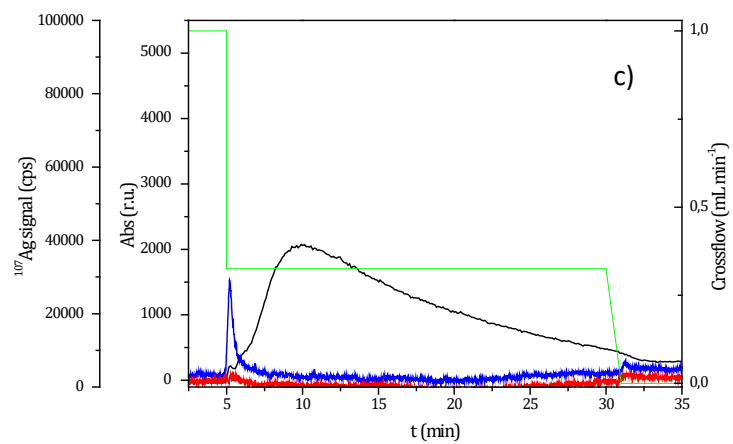


Figure 3

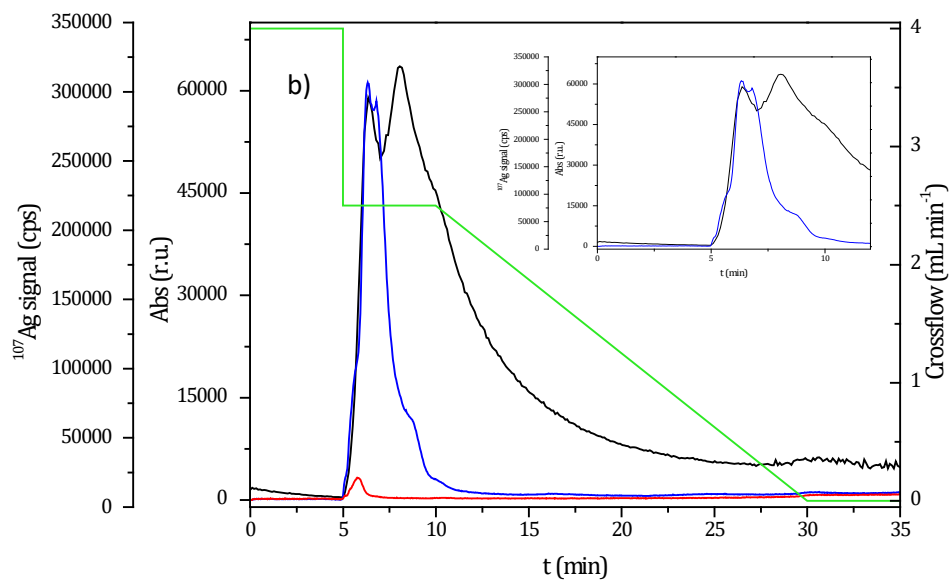
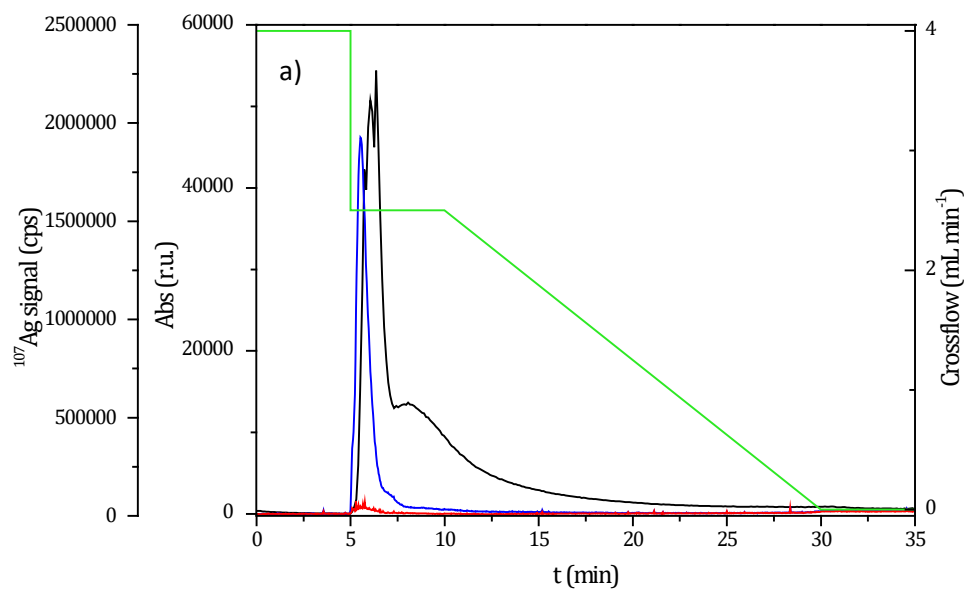


Table 1

AF4 crossflow programs. Out flow: 1.00 mL min⁻¹.

Program step	Time /min	Crossflow	
		Mode	mL min ⁻¹
Program A: low crossflow			
Injection/focusing	5	(Injection flow, 0.2 mL min ⁻¹)	1
Separation	25	Constant	0.325
	1	Linear decay	0.325 to 0
	4	Constant	0
Program B: high crossflow			
Injection/focusing	5	(Injection flow, 0.2 mL min ⁻¹)	4
Separation	5	Constant	2.5
	20	Linear decay	2.5 to 0
	5	Constant	0

Table 2

Percentage of silver mobilised (<0.5 µm) recovered after centrifugation or centrifugation followed by ultrafiltration in ultrapure water respect to the total silver content in the materials. Average ± standard deviation (n=3).

Composite	% Total Ag mobilised	% Ag < 3 kDa of Ag mobilised
Kaolinite-Ag	40 ± 2	91 ± 5
Sepiolite-Ag	48 ± 1	53 ± 2

Table 3

Percentage of silver mobilised (<0.5 μm) in each step of the *in vitro* digestibility assay respect to the total silver content in the materials. Average \pm standard deviation (n=3).

Composite	Step	% Total Ag mobilised	% Ultrafiltered Ag mobilised
Kaolinite-Ag	1	0.88 \pm 0.05	0.38 \pm 0.01
	2	17.21 \pm 0.13	0.82 \pm 0.10
	3	10.16 \pm 0.71	1.94 \pm 0.05
Sepiolite -Ag	1	1.31 \pm 0.10	0.78 \pm 0.02
	2	4.51 \pm 0.25	1.67 \pm 0.03
	3	7.31 \pm 0.07	3.81 \pm 0.16

Table 4

Total silver content ($\mu\text{g g}^{-1}$) of the lyophilized liver and muscle tissues and faeces from pigs. Average \pm standard deviation. P value represents the level of significance. (P<0.05 significant).

Treatment	Control	Kaolinite-Ag	Sepiolite-Ag	P	
	$\mu\text{g Ag g}^{-1}$	$\mu\text{g Ag g}^{-1}$	$\mu\text{g Ag g}^{-1}$		
Liver	Day 14	< 0.009 (n = 2)	4.8 \pm 1.4 (n = 6)	3.6 \pm 1.6 (n = 6)	0.19
	Day 62	< 0.009 (n = 4)	2.8 \pm 1.2 (n = 5)	2.2 \pm 0.6 (n = 5)	0.35
	P	-	0.04	0.11	
Faeces	Day 14	0.05 \pm 0.01 (n = 3)	114 \pm 29 (n = 4)	141 \pm 32 (n = 4)	0.25
	Day 62	n.d.	n.d.	n.d.	-
Muscle	Day 62	< 0.009 (n = 6)	< 0.009 (n = 6)	< 0.009 (n = 6)	-

n.d. not determined.

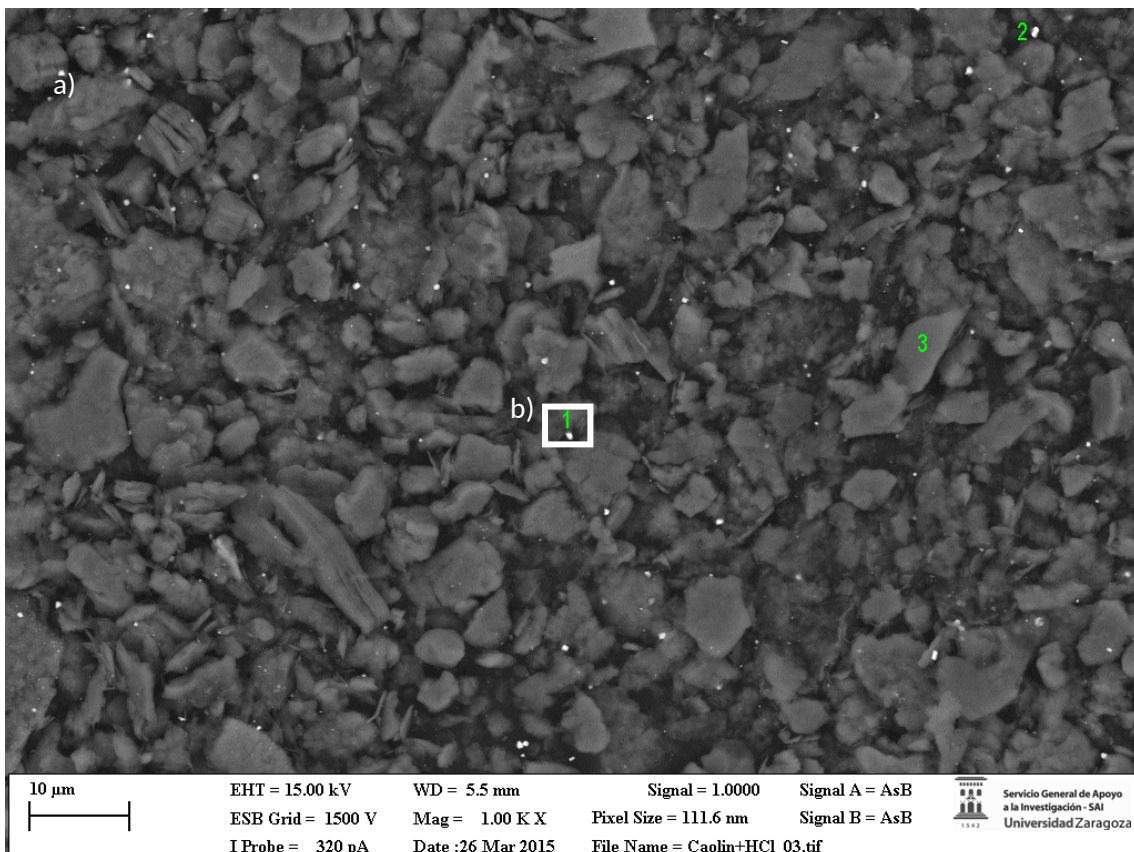
1 SUPPLEMENTARY INFORMATION FOR
2 SILVER NANOPARTICLE-CLAYS NANOCOMPOSITES AS FEED ADDITIVES:
3 CHARACTERIZATION OF SILVER SPECIES RELEASED DURING *IN VITRO* DIGESTIONS.
4 EFFECTS ON SILVER RETENTION IN PIGS

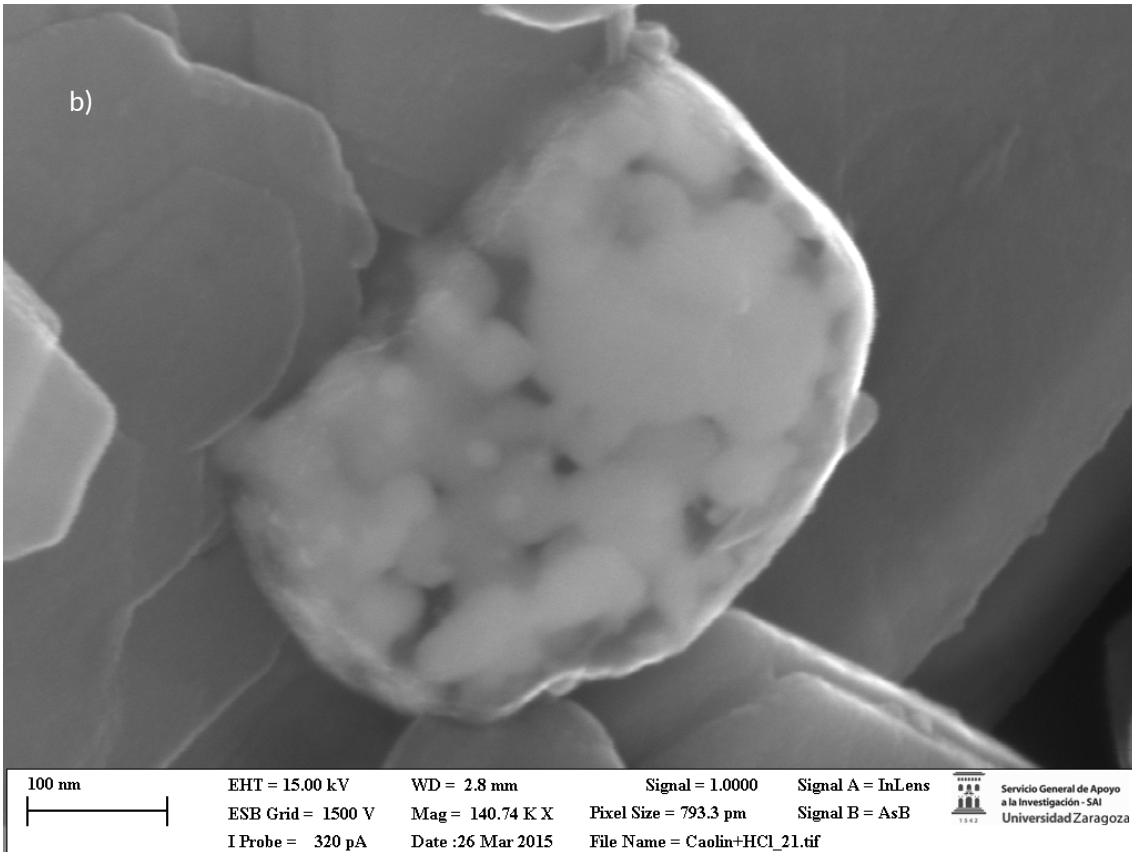
5 I. Abad-Álvarez¹, C. Trujillo¹, E. Bolea¹, F. Laborda¹, M. Fondevila², M.A. Latorre² and J.R.
6 Castillo¹

7 ¹ Group of Analytical Spectroscopy and Sensors (GEAS), Institute of Environmental Sciences
8 (IUCA), University of Zaragoza, Pedro Cerbuna 12, 50009 Zaragoza, Spain.

9 ² Departamento de producción Animal y Ciencia de los Alimentos, Instituto Agroalimentario de
10 Aragón (IA2), Universidad de Zaragoza-CITA, M. Servet 177, 50013 Zaragoza, Spain

11
12
13
14





1
2
3
4
5
6
7
8
9
10
11
12
13
14
15
16
17
18
19
20
21
22
23

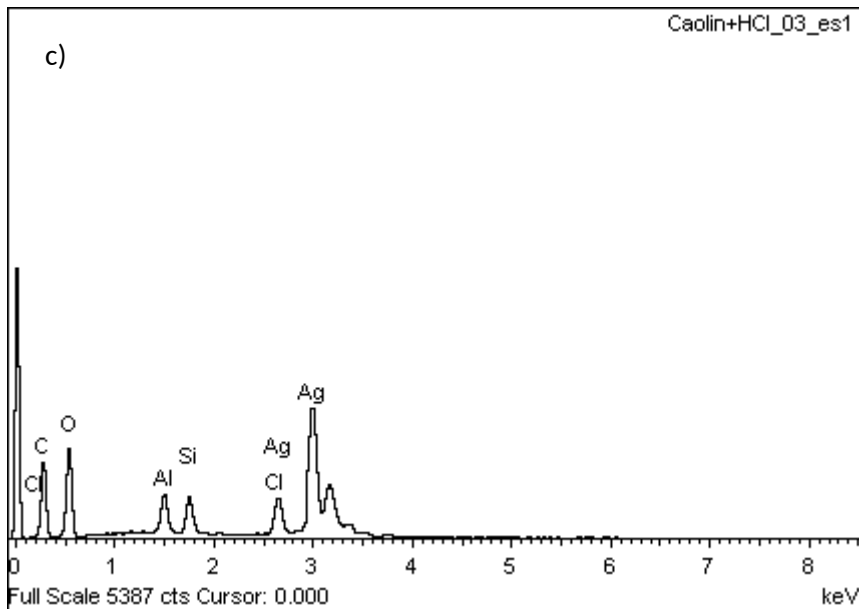
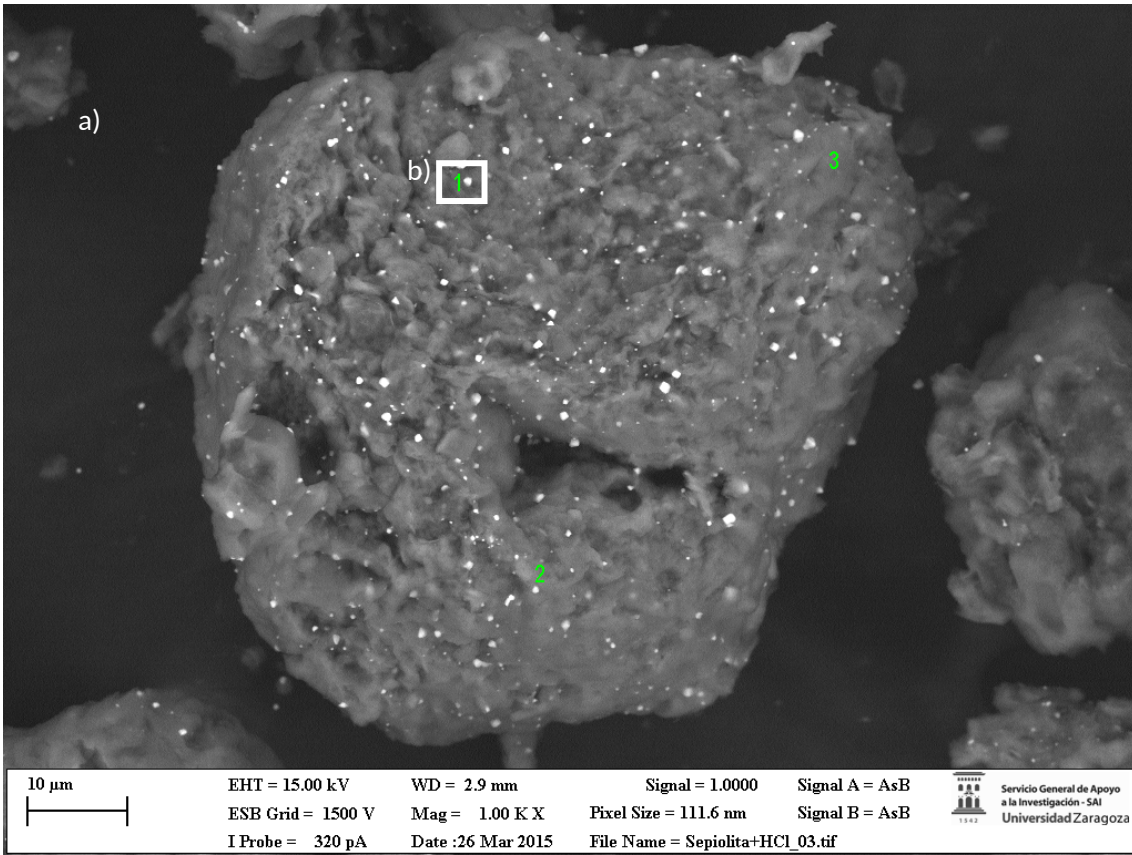
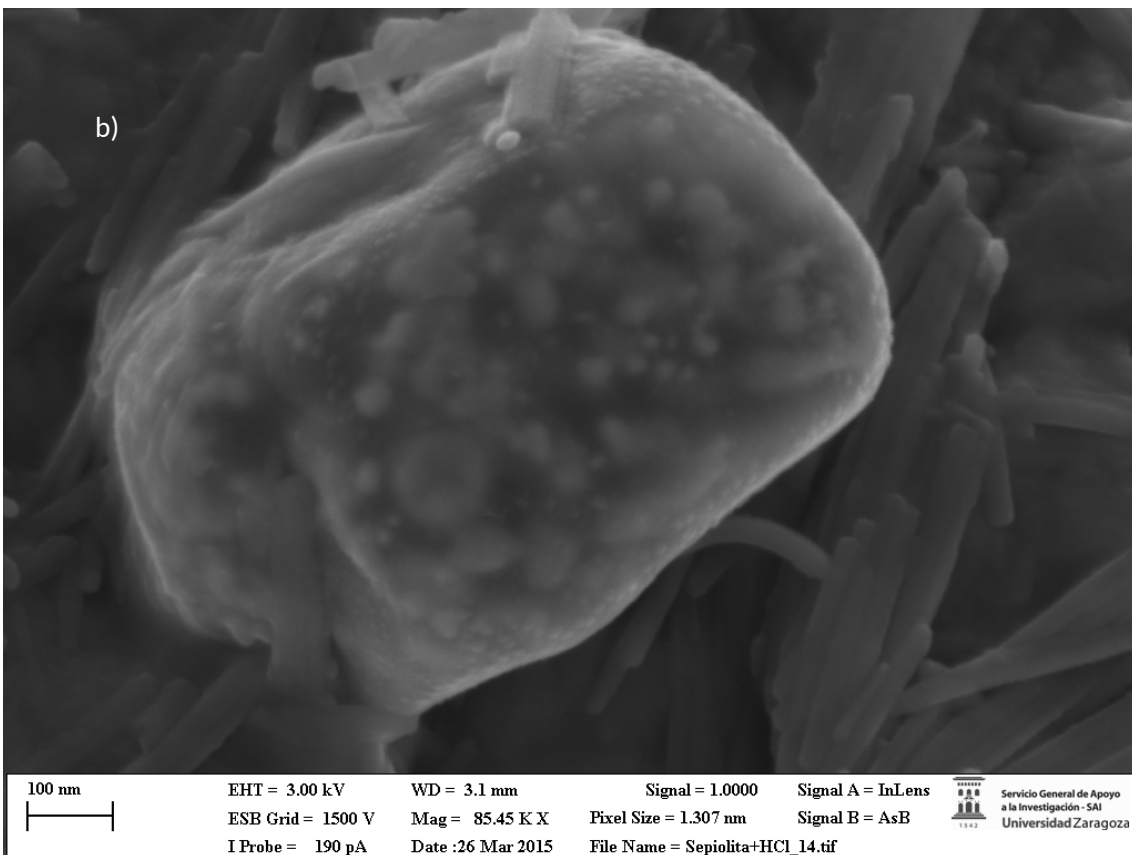


Figure S1 FESEM images. Microparticles of kaolinite-Ag a) with white spots on the surface (x1000) after treatment with HCl 0.01 M. b) Magnified micrograph from inset in a) (x140700). c) EDX spectra from white spots in a), point 1 in green.



1
2



3
4
5

1
2
3
4
5
6
7
8
9
10
11
12
13
14
15
16
17
18
19
20
21
22
23

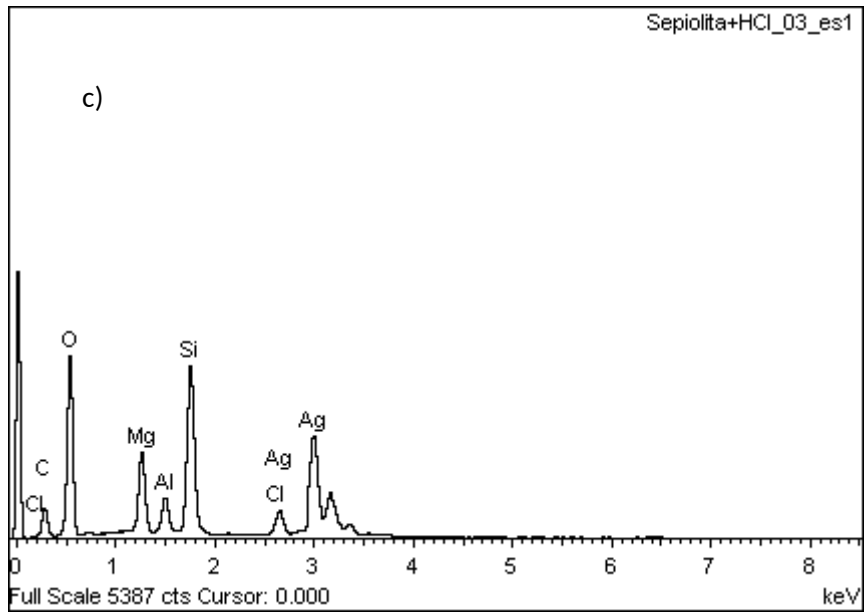
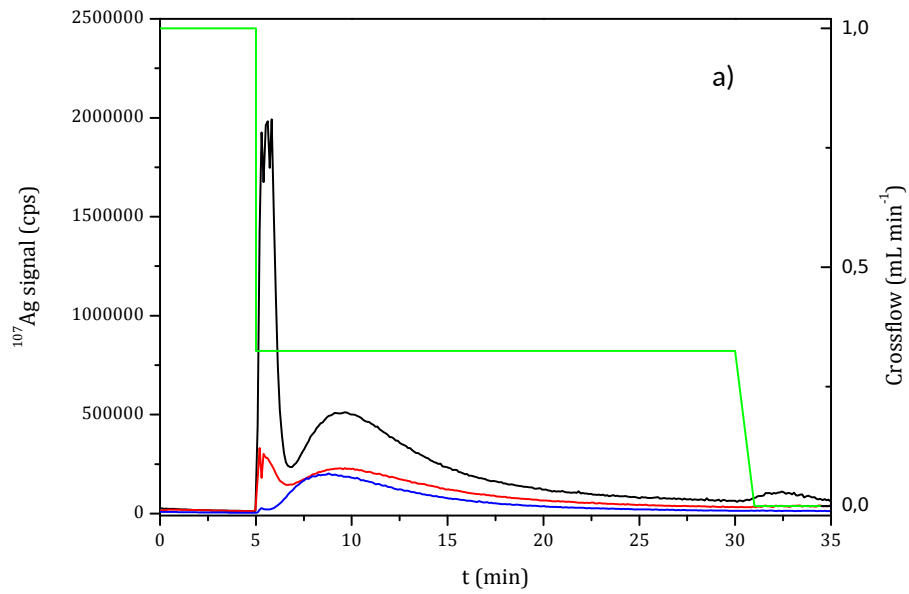
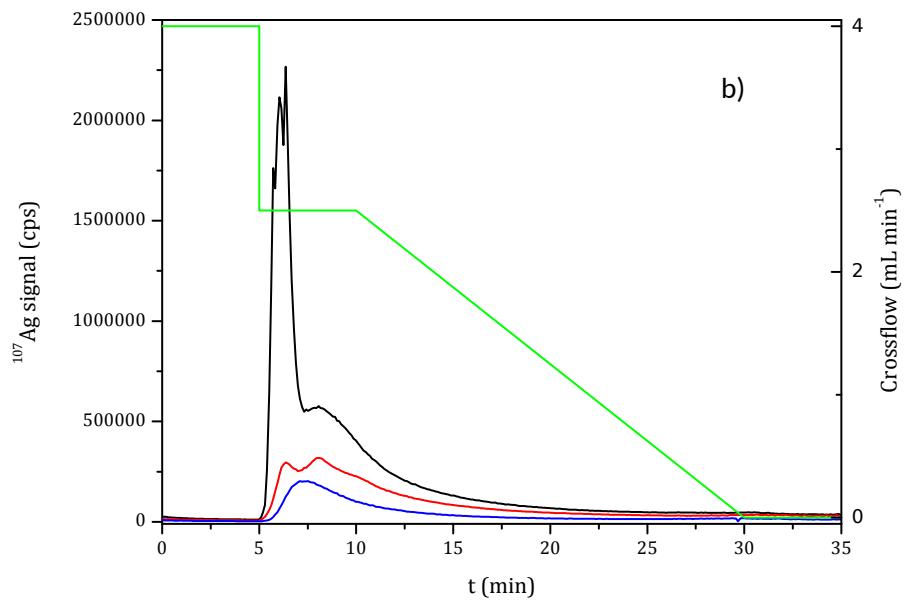


Figure S2 FESEM images. Microparticles of sepiolite-Ag a) with white spots on the surface (x1000) after treatment with HCl 0.01 M. b) Magnified micrograph from inset in a) (x85450). c) EDX spectra from white spots in a), point 1 in green.

1



2



3

4 **Figure S3** Comparison of the AF4-ICPMS fractograms of the suspensions from kaolin-Ag in
5 ultrapure water (blue), from Step 2 (black) and Step 3 (red) from an *in vitro* digestion process
6 using a) Crossflow program A (green line) and b) Crossflow program B (green line).

7

8